

# The Ultraviolet Environment of a Tropical Megacity in Transition: Mexico City 2000-2019

Adriana Ipiña<sup>1,2</sup>, Gamaliel López-Padilla<sup>3</sup>, Armando Retama<sup>4</sup>, Rubén D. Piacentini<sup>1</sup>, and Sasha Madronich<sup>5</sup>

<sup>1</sup>Instituto de Física Rosario (CONICET-UNR), Rosario, Argentina

<sup>2</sup>Centro de Ciencias de la Atmósfera, Universidad Nacional Autónoma de México, Mexico City, Mexico

<sup>3</sup>Facultad de Ciencias Físico Matemáticas, Universidad Autónoma de Nuevo León, San Nicolás de los Garza, México

<sup>4</sup>Independent researcher, Mexico City, Mexico

<sup>5</sup>National Center for Atmospheric Research, Boulder, Colorado, USA

## Abstract

Tropical regions experience naturally high levels of UV radiation, but urban pollution can reduce these levels substantially. We analyzed 20 years of measurements of the UV Index (UVI) at several ground-level locations in the Mexico City Metropolitan Area and compared these with UVI values estimated from satellite overpasses observing ozone and clouds (but not local pollution). The ground-based measurements were systematically lower than the satellite-based estimates, by ca. 40% in 2000 and 30% in 2019. Calculations with a radiative transfer model and observed concentrations of air pollutants explained well the difference between satellite- and ground-based UVI, and showed specific contributions from boundary layer aerosols, O<sub>3</sub>, NO<sub>2</sub>, and SO<sub>2</sub>, in decreasing order of importance. Such large changes in UV radiation have important implications ranging from human health (skin cancer and cataract induction) to air pollution control (photochemical smog formation).

Keywords: Ultraviolet radiation, UV Index, Megacities, Air pollution, Urban photochemistry.

Synopsis: Improvements in Mexico City's air quality during 2000-2019 were accompanied by increases in UV radiation, augmenting human exposure and photochemical smog formation.

## Introduction

Ultraviolet (UV) radiation is an important component of the urban environment, affecting human populations directly through UV exposure of skin and eyes<sup>1,2,3</sup> and less directly (but with great impact) by driving the

formation of photochemical smog, including tropospheric ozone and other oxidants, as well as secondary aerosols containing nitrates, sulfates, and organics.<sup>4,5,6</sup> These pollutants, along with others of primary origin commonly found in urban atmospheres (e.g., black carbon, sulfur dioxide), can in turn scatter and/or absorb UV radiation, alter its vertical distribution, and so modify the photochemical rate of their own formation. Such feedback complicates the calculation of both the UV radiation field (including at the surface), and the evolution of photochemical smog in the urban boundary layer.

The question of how air pollution alters the urban UV environment (and *vice versa*) is not new, but studies have relied mostly on numerical models,<sup>7,8,9</sup> with relatively fewer available observations (e.g., *McKenzie et al.*<sup>10</sup>; *Panicker et al.*<sup>11</sup>; *Palancar et al.*<sup>12</sup>; reviewed by Bais et al.<sup>13</sup>). Increases in UV have been estimated in association with decadal emission reductions, e.g. in China,<sup>14,15,16</sup> and have led to less-than-expected reductions in photochemical smog, in part due to stronger UV photochemistry.<sup>17,18,19</sup> Emission reductions have also occurred globally during the 2020 COVID-19 pandemic,<sup>20,21</sup> but ground-level ozone in polluted have actually increased,<sup>22,23</sup> due at least in part to the increased UV radiation. Unfortunately, the observational data base of relevant UV radiation remains rather sparse to evaluate such model-derived hypotheses.

The environment of Mexico City is of particular interest for several reasons: (1) Nearly 23 million people inhabit the Mexico City Metropolitan Area (MCMA), and the UV environment has direct implications for their health, both in terms of skin/eye UV exposure and *via* photochemical smog formation. (2) As a tropical megacity, it is to some extent representative of the situation of many others, with year-round intense midday UV irradiance, a shallower atmosphere due to significant elevation above sea level, and a transition toward newer and cleaner technologies, leading to gradual improvements in air quality. (3) Air quality within MCMA has undergone extensive scrutiny, with well-established monitoring network since 1986,<sup>24</sup> numerous intensive field campaigns to study the meteorology, emissions, and photochemistry of smog formation,<sup>25,26,27</sup> and numerical modeling incorporating the evolving knowledge.<sup>28,29,30,31</sup> This extensive body of knowledge provides the foundation for understanding our study.

Here, we analyze two decades of continuous measurements of the UV Index at multiple locations within the MCMA, collected by the Secretariat of the Environment (Secretaría del Medio Ambiente, SEDEMA) of the Mexico City government as part of an intensive monitoring network over the MCMA.<sup>32a</sup> The UV Index is defined as:

$$UVI = 40 \int_{250nm}^{400nm} E(\lambda, t) \cdot S_{er}(\lambda) d\lambda \quad (1)$$

where  $E(\lambda, t)$  is the solar spectral irradiance in units of  $\text{W}/(\text{m}^2 \cdot \text{nm})$  and  $S_{er}(\lambda)$  is the erythral sensitivity of human skin.<sup>33,34</sup> Multiplication by 40 is chosen historically to yield small integer scales, but is otherwise scientifically arbitrary.

The UVI is recognized by the World Health and Meteorological Organizations (WHO and WMO) as a standardized metric of UV radiation<sup>33</sup> for global public information. An advantage of using the UVI as (one) metric of UV radiation is that it is being increasingly observed or calculated and disseminated, enabling more objective comparisons between seasons and locations. The UVI observations from Mexico City, considered here, are an important element of this global picture.

While the UVI at the surface cannot be translated directly into photolysis frequencies for various photolabile molecules, the spectral weighting of the UVI (ca. 300-320 nm) is approximately similar to that for the photolysis of ozone to singlet oxygen atoms. Other UV wavelengths are of course also important, e.g. for the photolysis of nitrogen dioxide, and may be affected differently depending on the pollutant. With these considerations and a few other *caveats*, UVI trends examined here can also be used to infer accompanying trends in photolysis frequencies.

## Methods

### Ground-based measurements

The Mexico City Metropolitan Area is located at 19.4°N, 99.1°W, 2240 meters above sea level (asl), surrounded by mountain ridges exceeding 5000 m asl, with complex topography and thermal inversions that inhibit winds and favor intense air pollution.<sup>35,36</sup> Air quality monitoring and surface meteorological measurements in the MCMA are conducted continuously by the Atmospheric Monitoring System (SIMAT, by its Spanish acronym) of the Mexico City Government. Since the year 2000, UV radiometers (model 501-A, Solar Light Company Inc., Glenside, PA) detecting wavelengths between 280-400 nm have been measuring erythemally-weighted solar radiation. The calibrations were carried out annually, using a periodically calibrated reference sensor from the same manufacturer. Although at the beginning only a few stations were in operation and have been changing, currently 11 stations are recording erythral irradiances, which are then multiplied by 40 (see Eq. 1) to give UV Indices. Table 1 describes the location of the stations where UV Index has been measured. Figure 1 shown the radiometers of the SIMAT have been distributed over MCMA, prioritizing the sites with more density of population. Near real-time data for each station are available on the SIMAT official website <http://www.aire.cdmx.gob.mx/default.php>.

Station	Environment	Lat (°N)	Lon (°W)	El (masl)
CHO	school zone	19.27	99.89	2253
CUT	ecological park	19.72	99.20	2263
FAC	urban	19.48	99.24	2299
HAN	urban	19.42	99.08	2235
LAA	urban	19.48	99.15	2255
MER	downtown	19.42	99.12	2245
MON	rural	19.46	98.90	2252
MPA	rural	19.18	98.99	2594
PED	residential	19.33	99.20	2326
SAG	urban	19.53	99.03	2241
SFE	residential	19.36	99.26	2599
TLA	urban	19.53	99.20	2311
CCA	University city	19.33	99.18	2294

Table 1: SIMAT stations, environmental descriptors and geographical positions. Abbreviations names: Chalco (CHA), Cuautitlán (CUT), FES Acatlán (FAC), Hangares (HAN), Laboratorio de Análisis Ambiental (LAA), Merced (MER), Montecillo (MON), Milpa Alta (MPA), Pedregal (PED), San Agustín (SAG), Santa Fe (SFE), Centro de Ciencias de la Atmósfera (CCA) and Tlalnepantla (TLA).

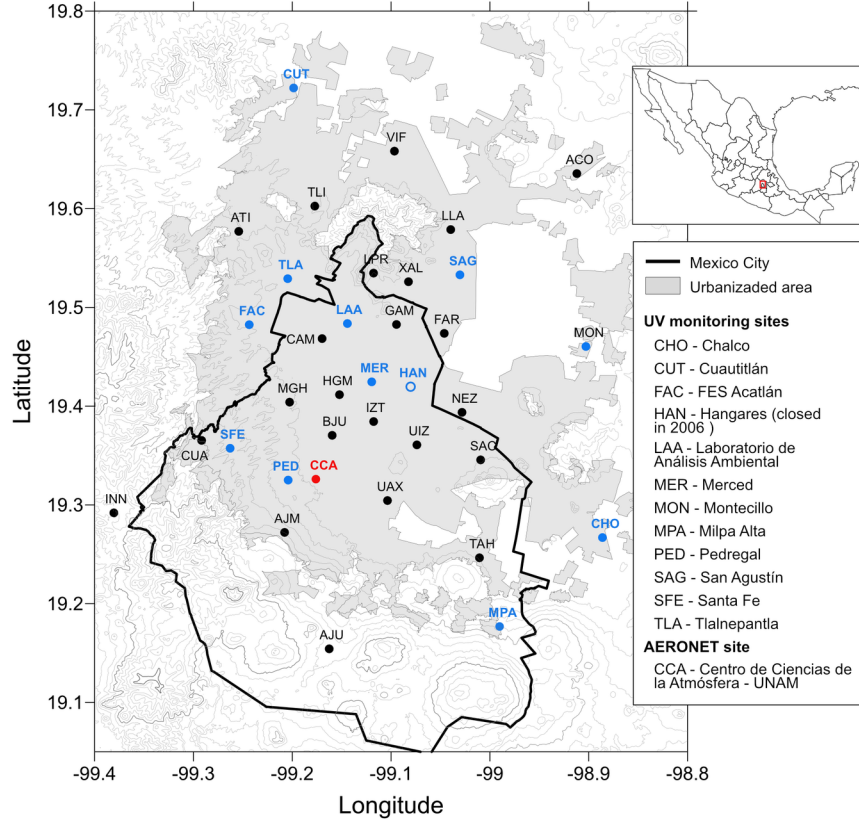


Figure 1: Map with the location of the SIMAT continuous monitoring stations over MCMA. Sites denoted by the blue solid dots correspond to the sites where UV had been measured, the site on open blue dot denoted a discontinued site, the red dot corresponds to the location of the AERONET site. The location of Mexico City and the acronyms of the UV and AERONET site are shown at the upper and lower frames at the right, respectively.

With the aim to explore the relationship between UVI and air pollutants levels, the hourly averages for ozone ( $O_3$ ), carbon monoxide (CO), nitrogen dioxide ( $NO_2$ ), sulfur dioxide ( $SO_2$ ) and particle matter with diameter sizes  $\leq 10$  micrometers ( $PM_{10}$ ), were downloaded from the SIMAT<sup>37</sup>. Only values obtained between 11h and 14h CST were considered for the trends analysis. Pollutants measurements are conducted by the SIMAT using regulatory-grade commercial instruments. Measurement principles include ultraviolet photometry (model 400E, Teledyne-API) for  $O_3$ , chemiluminescence (model 200E, Teledyne-API) for  $NO_2$ , UV fluorescence (model 100E, Teledyne API) for  $SO_2$ , and infrared absorption (model 300E, Teledyne-API) for CO. The  $PM_{10}$  continuous mass concentration was measured with Tapered Element Oscillating Microbalance (TEOM 1400AB or TEOM 1405 DF, Thermo Scientific) monitors. Gaseous pollutant levels

are reported in ppb concentration units for  $\text{O}_3$ ,  $\text{SO}_2$  and  $\text{NO}_2$ , and in ppm for CO. Particulate matter mass concentration is reported in  $\mu\text{g m}^{-3}$  at local conditions for temperature and pressure.

Aerosol optical depth at 340 nm was obtained from the Centro de Ciencias de la Atmósfera (CCA), measurements were conducted with a photometer of the Aerosol RObotic NETwork (AERONET<sup>38</sup>). The data Product Level 2.0 were selected, and annual averages  $\text{AOD}_{340}$  were calculated from continuous measurements during at least 7 months.

## Satellite data

Estimates of the UV Index from satellite-based measurements of clouds and  $\text{O}_3$  were used for comparing to the ground-based measurements. These data were provided by the Ozone Monitoring Instrument (OMI) on board of AURA-NASA satellite.<sup>39</sup> OMI was created in cooperation between the Netherlands Agency for Aerospace Programmes (NIVR), the Finnish Meteorological Institute (FMI) and NASA. OMI (hereafter OMI-Aura/NIVR-FMI-NASA) performs observations over a geographical dimension of  $13 \times 24\text{km}^2$  at nadir. For Mexico City, the satellite overpass time is between 19:00h - 21:00h UTC and data are specific for the coordinates and elevation of Mexico City. To our knowledge, no correction is made for local air pollution.

## TUV model

Calculations of the UV Index were also made with the Tropospheric Ultraviolet Visible (TUV v5.3) model.<sup>40</sup> The model vertical structure was modified to place the surface at 2.24 km asl, overlain by a 3 km boundary layer<sup>41,36</sup> in which the aerosol optical depth (AOD) and the concentrations of gaseous  $\text{O}_3$ ,  $\text{NO}_2$ , and  $\text{SO}_2$  can be varied. Above the atmospheric boundary layer (ABL) (i.e. above 5.24 km asl) the model defaults to a climatological continental aerosol profile<sup>42</sup> whose remaining optical depth (i.e. from 5.24 km to space) is 0.23 at 340 nm, and  $\text{O}_3$  profile from the US Standard Atmosphere with the total ozone column scaled to a climatological value of 265 Dobson Units. ABL aerosols are modeled by prescribing the AOD at 340 nm (from AERONET observations), scaled to other wavelengths inversely with wavelength (Angstrom coefficient = 1.0), asymmetry factor of 0.7, and a single scattering albedo of 0.85 at UV wavelengths, following the determinations made in Mexico City by Corr et al.<sup>43</sup> and Palancar et al.<sup>12</sup>. Radiative transfer calculations were carried out with the pseudo-spherical 4-stream option.

## Results and Discussion

Figure 2 shows the diurnal variation of the UVI for several specific cloud-free days, for different seasons and several locations. Peak values range from 8 during autumn/winter to almost 12 in spring/summer, in correspondence to the respective December and June solstices, and follow closely the yearly variation of the cosine of the solar zenith angle at noon (see Figure 4). Although the stations are all within a 25 km radius, substantial differences among them are notable. The differences are particularly evident in the afternoons, when air pollutants have significantly accumulated within the boundary layer and the mixing height is maximum, suggesting that their origin is not related to calibration biases between the instruments. Survey of the locations revealed that shadowing from nearby structures is not an issue. It is more likely that local differences in air pollution, particularly aerosols, are the cause of this variability. Previous studies (e.g., Castro et al.<sup>44</sup> and Palancar et al.<sup>12</sup>) have shown that surface UV radiation in Mexico City is attenuated significantly by aerosols. The measurements shown in Fig 2 are consistent with increasing pollution during the course of the day, with highest aerosol loading (and highest variability) attained in the afternoon. Further support for the role of pollution in suppressing the UVI comes from the observation made at Santa Fe (SFE) site which in Fig. 2 are seen to be systematically higher, e.g. by over 10% in autumn afternoons, compared to the other stations. The SFE station is located at 2600 m asl, approximately 300 m higher than Mexico City downtown, and so avoids a substantial fraction of the polluted MCMA boundary layer.<sup>45</sup> It is indeed expected to have higher values of the UVI, in agreement with the observations.

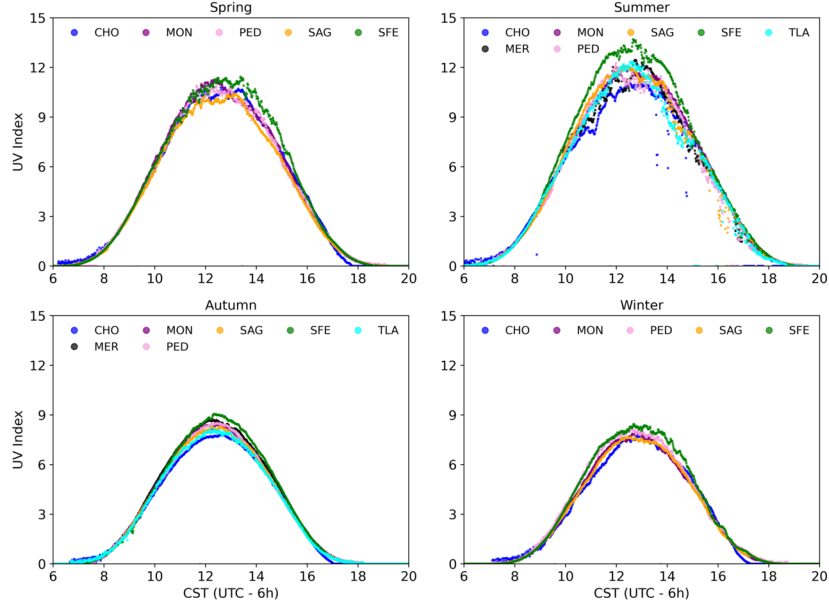


Figure 2: UV Index measured over MCMA by SIMAT stations each minute along the day under cloudless conditions for the seasons and dates (month/day/year): Spring (04/20/2018), Summer (06/23/2018), Autumn (11/13/2018) and Winter (02/02/2018).

126 Daily maximum values,  $UVI_{\max}$ , were extracted from the time interval 11:00 h-14:00 h CST from each of the  
 127 stations, with 7305 continuous days of measurements, during the period 2000-2019. As shown in Figure 3,  
 128 these values ranged from 1 to 15, with a majority (62%) of the days experienced  $UVI_{\max}$  values between 6  
 129 and 10, and remarkably few, less than 1%, in the higher 13-15 range.



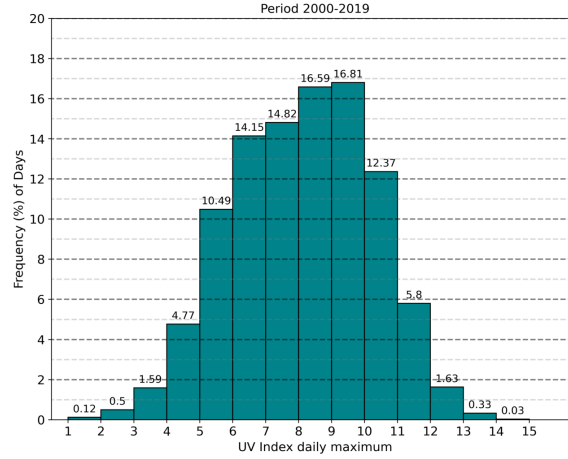


Figure 3: Frequency distribution of daily maximum UV Index values in Mexico City during 2000 -2019.

130 Similar patterns are found when considering the monthly averages ( $\overline{UVI}_m$ ) of daily  $UVI_{\max}$  as shown in  
 131 Figure 4. The long-term averages present a seasonal variation (as in Fig. 2), following approximately the  
 132 cosine of the noontime solar zenith angle. Notably, values rarely if ever exceed 12 (as in Fig. 3). Long term  
 133 trends in  $\overline{UVI}_m$  are shown in Figure 5. A clear upward trend is seen, with a slope for the linear fit of  
 134 0.7%/year or +1.2 UVI units over the two decades.

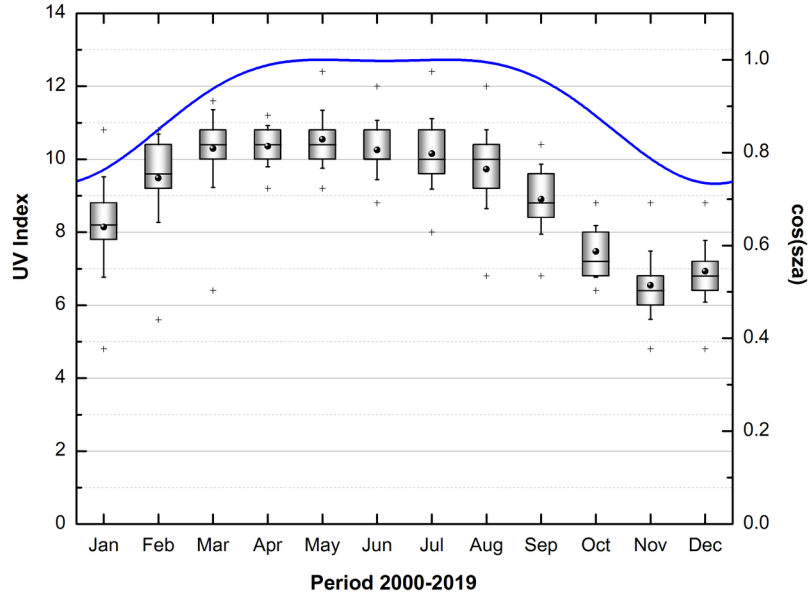


Figure 4: Boxplot of monthly UV Index in MCMA for the period 2000-2019: median (central bold line), average (black dot), 25<sup>th</sup> and 75<sup>th</sup> percentiles (box edges), standard deviation (the whiskers), the minimum and maximum values (plus sign) and the cosine of the solar zenith angle at solar noon (blue curve).

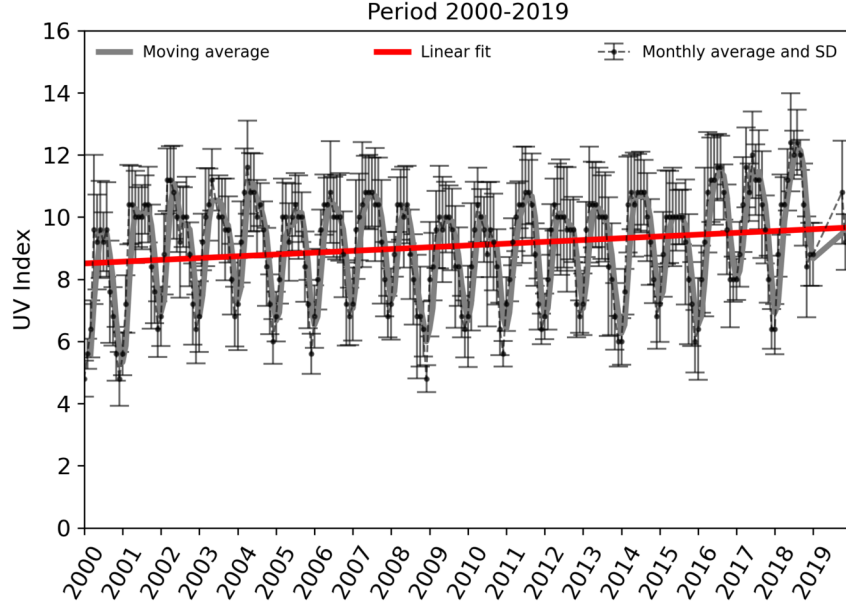


Figure 5: Moving average function (gray curve) applied to monthly average UV Index, standard deviation (black dots and dash line) and linear fit (red line).

The UV Index computed from satellite-based observations (OMI-Aura/NIVR-FMI-NASA) over the period 2005-2019 is mapped in Figure 6. The satellite-derived UVIs vary from 8 in winter to 15 in summer, both values being substantially higher than the ground-based observations (ca. 6 for winter and 11 for summer, see Fig. 4). We hypothesize that this large difference between satellite-based estimation and ground-based observation of the UV index is due to the intense air pollution of Mexico City. A rather similar behavior was detected in Santiago city, Chile.<sup>46</sup>

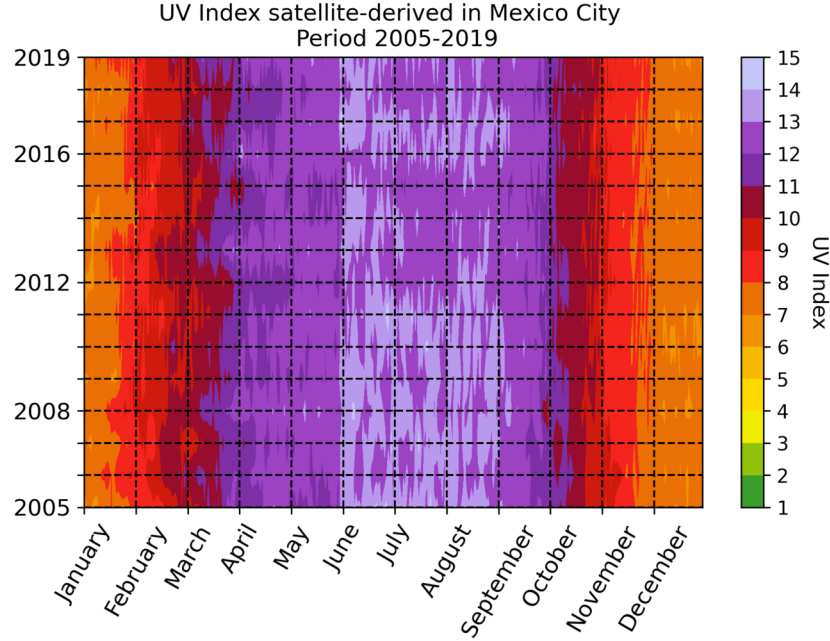


Figure 6: UV Index recorded by OMI-Aura/NIVR-FMI-NASA, from 2005 to 2019.

## Effect of pollutants on UV radiation

Trends and averages in aerosol optical depth  $AOD_{340}$  and criteria pollutants  $PM_{10}$ ,  $CO$ ,  $NO_2$ ,  $O_3$  and  $SO_2$  observed at the SIMAT stations over 2000-2019, are shown in Figure 7 and summarized in Table 2 together with the  $UVI_{max}$ . Similar trends have been noted before<sup>47,48,49</sup> and reflect the long-term success of emission reduction policies and programs.

The observed changes in the concentrations of these air pollutants have significant implications for surface UV radiation, as can be demonstrated with the TUV radiative transfer model (see Table 3). The UVI under an ideally clear atmosphere would reach 15.9 (at noon on 21 June), but pollutant concentrations in the year 2000 (estimated from Table 2 and Fig. 7) reduce the UVI by nearly 40%, down to 9.7. Most of this reduction is due to aerosols in the ABL, with additional contributions from aerosols in the free troposphere (FT), and ABL gaseous  $O_3$ ,  $NO_2$ , and  $SO_2$  in order of decreasing importance. The pollution-related UV reductions in 2019 are less severe, with UVI increasing by 14% to 11.1 over the two decades, but still 30% below values of ideally clean skies. Thus, the model calculations for clear skies are in good agreement with the satellite-derived UVI values, and the model calculations with observed pollutants are in good agreement with ground-based UVI values, even reflecting their long-term trend.

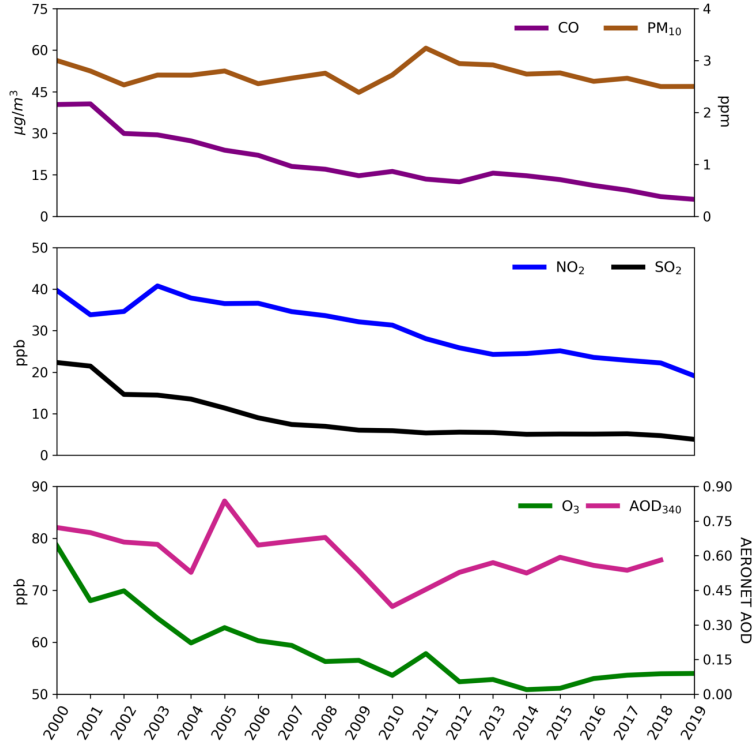


Figure 7: Air quality trends in MCMA for the period 2000-2019 from annual averages obtained between 11h to 14h CST every day: PM<sub>10</sub> (brown curve), CO (purple curve), NO<sub>2</sub> (blue curve), SO<sub>2</sub> (black curve), O<sub>3</sub> (green curve) and AOD<sub>340</sub> (pink curve).

Variable	$\frac{\Delta variable}{\Delta t}$	Avg <sub>2000-2019</sub>	$\Delta(\%/year)$
UVI	0.06	9.1	0.7
PM <sub>10</sub>	-0.12	51.1	-0.2
CO	-0.08	1.0	-8.2
NO <sub>2</sub>	-1.04	30.4	-3.4
O <sub>3</sub>	-1.05	58.5	-1.8
AOD <sub>340</sub>	-0.01	0.6	-1.6
SO <sub>2</sub>	-0.82	8.9	-9.2

Table 2: UV Index and criteria pollutants: slope for the period 2000-2019, averages in units of  $\mu g/m^3$  (PM<sub>10</sub>), ppm (CO), ppb (SO<sub>2</sub>, NO<sub>2</sub> and O<sub>3</sub>), dimensionless (UV Index and AOD<sub>340</sub>) and annual percentage change (%/year).

Comparable UV reductions, of 30-40% due to aerosols, were reported by Panicker et al.<sup>11</sup> over Pune, India from April 2004 to March 2005, with sensitivity coefficients (i.e. change in UVI per unit change in AOD) similar to those found here in Table 3. Over Europe, ground-based UVI observations for several decades are systematically lower than those estimated from satellites even after consideration of climatological aerosol distributions, showing the importance of local pollution not resolved from space.<sup>50</sup>

Conditions	UV Index at Noon 21 June	Description
Clean PBL	15.9	
Year 2000 - Aerosols AOD: 0.23 in FT, 0.7 in PBL; O <sub>3</sub> =70, NO <sub>2</sub> =40, SO <sub>2</sub> =10 ppb	9.7	-6.2 (a 39% reduction from clean atmosphere)
Excluding FT aerosols	10.8	+1.1
Excluding PBL aerosols	12.7	+3.0
Excluding PBL O <sub>3</sub>	10.4	+0.7
Excluding PBL NO <sub>2</sub>	10.1	+0.4
Excluding PBL SO <sub>2</sub>	9.9	+0.2
Year 2019 - Aerosol AOD: 0.23 in FT, 0.5 in PBL; O <sub>3</sub> =50, NO <sub>2</sub> =20, SO <sub>2</sub> =1 ppb	11.1	+1.4 (relative to 2000) a 14% increase; +4.8 (relative to clean atmosphere) still 30% reduction from clean atmosphere

Table 3: TUV Model Calculation Illustrating the Effect of Pollutants on the UV Index in Mexico City. The contribution of each pollutant is evaluated by subtraction from the full mixture, rather than individual additions to clean air, to represent more faithfully the interaction between scattering and absorption, e.g. scattering-induced changes in photon path lengths through absorbing gases.

UV reductions by air pollutants are expected to be most severe near the surface. Thus, such reductions cannot be applied directly to the photochemical processing that occurs throughout the ABL. If the aerosols are optically thin and moderately absorbing (as is the case here), the reduction in vertically averaged UV can be estimated crudely as half of the reduction seen at the surface (e.g., Castro et al.<sup>44</sup>, see their Fig. 7). However, scattering complicates the situation, and a full radiative transfer calculation is preferable to such crude estimates, with the observed surface UVI used to anchor the model at the lower boundary.

An issue that is beginning to gain relevance in radiative balance models is the influence of a group of organic compounds capable of strongly absorbing in the UV region (brown carbon).<sup>51</sup> Some of these compounds are related with emissions from local and regional wildfires.<sup>52</sup> Mexico City is frequently exposed to regional fire smoke transport during the dry part of the year (November to May)<sup>53</sup>, that sporadically modify the optical properties of the aerosols.<sup>54</sup> This could partly explain the relatively minor reductions in PM<sub>10</sub> (see Fig. 7), compared to the larger reductions of CO, NO<sub>2</sub>, and O<sub>3</sub> that are more directly related to urban activities, as well as some of the seasonal asymmetry seen in Fig. 3.

The UVI is specific to wavelengths mainly in the 300-320 nm range, and so the question remains whether these results can be applied at longer UV wavelengths, e.g. those important for NO<sub>2</sub> photolysis (<420 nm). Absorption by SO<sub>2</sub> and O<sub>3</sub> vanishes, while absorption by NO<sub>2</sub> increases and typical aerosols optical depth decrease. These changes can easily be modeled, but unfortunately far fewer measurements of these longer wavelengths are available in Mexico City or elsewhere.

## Conclusion

Two decades of observations in Mexico City demonstrate unequivocally that air pollution reduces UV radiation at the ground. The ground-based observations are well below estimates derived from satellite-based observations, and below model calculations do not consider optically important pollutant aerosols, tropospheric ozone, and to a lesser extent NO<sub>2</sub> and SO<sub>2</sub>. When typical observed values of these pollutants are included in a model (e.g. TUV), the differences between satellite-derived and ground-based measured values are explained and can be attributed quantitatively to individual observed pollutants. Long term improvements in air quality, over two decades, are accompanied by statistically significant increases in the observed UVI, again in good agreement with the model-predicted changes.

The reductions in surface UV radiation with respect to an ideally clear atmosphere – by 40% in 2000 and still 30% in 2020 – are large, be it the context of human UV exposure or air quality mitigation. In urban areas where ozone production scales proportionally with UV levels and with volatile organic compound (VOC) emissions (the VOC-limited regime), a 20% increase in average UV means that VOC emissions will need to be reduced by 20% to meet the same values, or else successful reductions in aerosols would lead to unwanted UV-driven increases in O<sub>3</sub>. Given the importance of the formation of photochemical secondary compounds in the degradation of the air quality, it is advisable to extend a study of the impacts in the changes of actinic flux. The efforts that Mexico City has made to improve air quality have achieved positive results

in the levels of most air pollutants. Nevertheless, ironically they caused an increase in UV radiation that reaches the surface, which could have consequences on human health. For human exposure, a 30% increase in UV-induced skin cancer and cataract would constitute a non-negligible public health issue and require a reassessment of preventive behaviors.

A limitation of the present work is our focus on daily maximum values, which largely exclude cloud cover. Absorption within clouds can be enhanced by the long path lengths of multiply scattered photons (e.g., Mayer et al.<sup>55</sup>, so that accurate quantification of UV effects of clouds in polluted environments remains a significant challenge and interesting opportunity for future work.

## Acknowledgements

We wish to acknowledge the staff of SIMAT, from the Secretariat of Environment, for the data and the continuous assistance during the realization of this project. Adriana Ipiña would like to extend her thanks to Dirección General de Personal Académico, Universidad Nacional Autónoma de México (DGAPA-UNAM) for the postdoctoral fellowship at Centro de Ciencias de la Atmósfera of the UNAM. Rubén D Piacentini wishes to thank CONICET and National University of Rosario, Argentina, for their partial support to the present work. The National Center for Atmospheric Research is sponsored by the National Science Foundation.

## References

- [1] Hugh R. Taylor, Sheila K. West, Frank S. Rosenthal, Beatriz Muñoz, Henry S. Newland, Helen Abbey, and Edward A. Emmett. Effect of Ultraviolet Radiation on Cataract Formation. *New England Journal of Medicine*, 319(22):1429–1433, dec 1988. URL <https://doi.org/10.1056%2Fnejm198812013192201>.
- [2] C. Varotsos and E. Feretis. Health effects on human eye resulting from the increased ambient solar ultraviolet radiation. *Toxicological & Environmental Chemistry*, 61(1-4):43–68, aug 1997. URL <https://doi.org/10.1080%2F02772249709358473>.
- [3] R. M. Lucas, S. Yazar, A. R. Young, M. Norval, F. R. de Gruijl, Y. Takizawa, L. E. Rhodes, C. A. Sinclair, and R. E. Neale. Human health in relation to exposure to solar ultraviolet radiation under changing stratospheric ozone and climate. *Photochemical & Photobiological Sciences*, 18(3):641–680, 2019. URL <https://doi.org/10.1039%2F8pp90060d>.



- [4] Philip A. Leighton. Physical Chemistry. In *Photochemistry of Air Pollution*, pages v–vi. Elsevier, 1961. URL <https://doi.org/10.1016%2Fb978-0-12-442250-6.50004-3>.
- [5] John H. Seinfeld, Spyros N. Pandis, and Kevin Noone. Atmospheric Chemistry and Physics: From Air Pollution to Climate Change. *Physics Today*, 51(10):88–90, oct 1998. URL <https://doi.org/10.1063%2F1.882420>.
- [6] Barbara J. Finlayson-Pitts and James N. Pitts. Theory, Experiments, and Applications. In *Chemistry of the Upper and Lower Atmosphere*, pages xvii–xviii. Elsevier, 2000. URL <https://doi.org/10.1016%2Fb978-012257060-5%2F50000-9>.
- [7] S. C. Liu, S. A. McKeen, and S. Madronich. Effect of anthropogenic aerosols on biologically active ultraviolet radiation. *Geophysical Research Letters*, 18(12):2265–2268, dec 1991. URL <https://doi.org/10.1029%2F91gl02773>.
- [8] Ali A. Sabziparvar, Piers M. F. Forster, and Keith P. Shine. Changes in ultraviolet radiation due to stratospheric and tropospheric ozone changes since preindustrial times. *Journal of Geophysical Research: Atmospheres*, 103(D20):26107–26113, oct 1998. URL <https://doi.org/10.1029%2F98jd02277>.
- [9] Sasha Madronich, Mark Wagner, and Philip Groth. Influence of Tropospheric Ozone Control on Exposure to Ultraviolet Radiation at the Surface. *Environmental Science & Technology*, 45(16):6919–6923, aug 2011. URL <https://doi.org/10.1021%2Fes200701q>.
- [10] R. L. McKenzie, C. Weinreis, P. V. Johnston, B. Liley, H. Shiona, M. Kotkamp, D. Smale, N. Takegawa, and Y. Kondo. Effects of urban pollution on UV spectral irradiances. *Atmospheric Chemistry and Physics*, 8(18):5683–5697, sep 2008. URL <https://doi.org/10.5194%2Facp-8-5683-2008>.
- [11] A. S. Panicker, G. Pandithurai, T. Takamura, and R. T. Pinker. Aerosol effects in the UV-B spectral region over Pune an urban site in India. *Geophysical Research Letters*, 36(10), may 2009. URL <https://doi.org/10.1029%2F2009gl0137632>.
- [12] G. G. Palancar, B. L. Lefer, S. R. Hall, W. J. Shaw, C. A. Corr, S. C. Herndon, J. R. Slusser, and S. Madronich. Effect of aerosols and NO<sub>2</sub> concentration on ultraviolet actinic flux near Mexico City during MILAGRO: measurements and model calculations. *Atmospheric Chemistry and Physics*, 13(2):1011–1022, jan 2013. URL <https://doi.org/10.5194%2Facp-13-1011-2013>.
- [13] A. F. Bais, R. L. McKenzie, G. Bernhard, P. J. Aucamp, M. Ilyas, S. Madronich, and K. Tourpali. Ozone

depletion and climate change: impacts on UV radiation. *Photochemical & Photobiological Sciences*, 14(1):19–52, 2015. URL <https://doi.org/10.1039%2Fc4pp90032d>.

[14] Michael Hollaway, Oliver Wild, Ting Yang, Yele Sun, Weiqi Xu, Conghui Xie, Lisa Whalley, Eloise Slater, Dwayne Heard, and Dantong Liu. Photochemical impacts of haze pollution in an urban environment. *Atmospheric Chemistry and Physics*, 19(15):9699–9714, aug 2019. URL <https://doi.org/10.5194%2Facp-19-9699-2019>.

[15] Ke Li, Daniel J. Jacob, Hong Liao, Lu Shen, Qiang Zhang, and Kelvin H. Bates. Anthropogenic drivers of 2013–2017 trends in summer surface ozone in China. *Proceedings of the National Academy of Sciences*, 116(2):422–427, dec 2018. URL <https://doi.org/10.1073%2Fpnas.1812168116>.

[16] Yonghong Wang, Wenkang Gao, Shuai Wang, Tao Song, Zhengyu Gong, Dongsheng Ji, Lili Wang, Zirui Liu, Guiqian Tang, Yanfeng Huo, Shili Tian, Jiayun Li, Mingge Li, Yuan Yang, Biwu Chu, Tuukka Petäjä, Veli-Matti Kerminen, Hong He, Jiming Hao, Markku Kulmala, Yuesi Wang, and Yuanhang Zhang. Contrasting trends of PM<sub>2.5</sub> and surface-ozone concentrations in China from 2013 to 2017. *National Science Review*, 7(8):1331–1339, feb 2020. URL <https://doi.org/10.1093%2Fnsr%2Fnwaa032>.

[17] Wenjie Wang, Xin Li, Min Shao, Min Hu, Limin Zeng, Yusheng Wu, and Tianyi Tan. The impact of aerosols on photolysis frequencies and ozone production in Beijing during the 4-year period 2012–2015. *Atmospheric Chemistry and Physics*, 19(14):9413–9429, jul 2019. URL <https://doi.org/10.5194%2Facp-19-9413-2019>.

[18] Jinhui Gao, Ying Li, Bin Zhu, Bo Hu, Lili Wang, and Fangwen Bao. What have we missed when studying the impact of aerosols on surface ozone via changing photolysis rates? apr 2020. URL <https://doi.org/10.5194%2Facp-2020-140>.

[19] Xiaodan Ma, Jianping Huang, Tianliang Zhao, Cheng Liu, Kaihui Zhao, Jia Xing, and Wei Xiao. Rapid increase in summer surface ozone over the North China Plain during 2013–2019: a side effect of particulate matters reduction control? jul 2020. URL <https://doi.org/10.5194%2Facp-2020-385>.

[20] M. Bauwens, S. Compernelle, T. Stavrou, J.-F. Müller, J. Gent, H. Eskes, P. F. Levelt, R. A. J. P. Veefkind, J. Vlietinck, H. Yu, and C. Zehner. Impact of coronavirus outbreak on NO<sub>2</sub> pollution assessed using TROPOMI and OMI observations. 47(11), jun 2020. URL <https://doi.org/10.1029%2F2020gl087978>.

[21] Zander S. Venter, Kristin Aunan, Sourangsu Chowdhury, and Jos Lelieveld. COVID-19 lockdowns cause

global air pollution declines. *Proceedings of the National Academy of Sciences*, 117(32):18984–18990, jul 2020. URL <https://doi.org/10.1073%2Fpnas.2006853117>.

[22] Xiaoqin Shi and Guy P. Brasseur. The Response in Air Quality to the Reduction of Chinese Economic Activities During the COVID-19 Outbreak. *Geophysical Research Letters*, 47(11), jun 2020. URL <https://doi.org/10.1029%2F2020gl088070>.

[23] Tianhao Le, Yuan Wang, Lang Liu, Jiani Yang, Yuk L. Yung, Guohui Li, and John H. Seinfeld. Unexpected air pollution with marked emission reductions during the COVID-19 outbreak in China. *Science*, 369(6504):702–706, jun 2020. URL <https://doi.org/10.1126%2Fscience.abb7431>.

[24] *Red Automática de Monitoreo Atmosférico (RAMA)*. URL <http://www.aire.cdmx.gob.mx/descargas/datos/excel/RAMAxls.pdf>. Accessed on Sat, December 05, 2020.

[25] J. C. Doran, S. Abbott, J. Archuleta, X. Bian, J. Chow, R. L. Coulter, S. F. J. de Wekker, S. Edgerton, S. Elliott, A. Fernandez, J. D. Fast, J. M. Hubbe, C. King, D. Langley, J. Leach, J. T. Lee, T. J. Martin, D. Martinez, J. L. Martinez, G. Mercado, V. Mora, M. Mulhearn, J. L. Pena, R. Petty, W. Porch, C. Russell, R. Salas, J. D. Shannon, W. J. Shaw, G. Sosa, L. Tellier, B. Templeman, J. G. Watson, R. White, C. D. Whiteman, and D. Wolfe. The IMADA-AVER Boundary Layer Experiment in the Mexico City Area. *Bulletin of the American Meteorological Society*, 79(11):2497–2508, 11 1998. ISSN 0003-0007. URL [https://doi.org/10.1175/1520-0477\(1998\)079<2497:TIABLE>2.0.CO;2](https://doi.org/10.1175/1520-0477(1998)079<2497:TIABLE>2.0.CO;2).

[26] L. T. Molina, C. E. Kolb, B. de Foy, B. K. Lamb, W. H. Brune, J. L. Jimenez, R. Ramos-Villegas, J. Sarmiento, V. H. Paramo-Figueroa, B. Cardenas, V. Gutierrez-Avedoy, and M. J. Molina. Air quality in North America's most populous city – overview of the MCMA-2003 campaign. *Atmospheric Chemistry and Physics*, 7(10):2447–2473, may 2007. URL <https://doi.org/10.5194%2Facp-7-2447-2007>.

[27] L. T. Molina, S. Madronich, J. S. Gaffney, E. Apel, B. de Foy, J. Fast, R. Ferrare, S. Herndon, J. L. Jimenez, B. Lamb, A. R. Osornio-Vargas, P. Russell, J. J. Schauer, P. S. Stevens, R. Volkamer, and M. Zavala. An overview of the MILAGRO 2006 Campaign: Mexico City emissions and their transport and transformation. *Atmospheric Chemistry and Physics*, 10(18):8697–8760, sep 2010. URL <https://doi.org/10.5194%2Facp-10-8697-2010>.

[28] Aron D. Jazcilevich, Agustín R. García, and Ernesto Caetano. Locally induced surface air confluence by complex terrain and its effects on air pollution in the valley of Mexico. *Atmospheric Environment*, 39(30):5481–5489, sep 2005. URL <https://doi.org/10.1016%2Fj.atmosenv.2005.05.046>.

- [29] Xuexi Tie, Sasha Madronich, GuoHui Li, Zhuming Ying, Renyi Zhang, Agustin R. Garcia, Julia Lee-Taylor, and Yubao Liu. Characterizations of chemical oxidants in Mexico City: A regional chemical dynamical model (WRF-Chem) study. *Atmospheric Environment*, 41(9):1989–2008, mar 2007. URL <https://doi.org/10.1016%2Fj.atmosenv.2006.10.053>.
- [30] Y. Zhang, M. K. Dubey, S. C. Olsen, J. Zheng, and R. Zhang. Comparisons of WRF/Chem simulations in Mexico City with ground-based RAMA measurements during the 2006-MILAGRO. *Atmospheric Chemistry and Physics*, 9(11):3777–3798, jun 2009. URL <https://doi.org/10.5194%2Facp-9-3777-2009>.
- [31] Miguel Zavala, William H. Brune, Erik Velasco, Armando Retama, Luis Adrian Cruz-Alavez, and Luisa T. Molina. Changes in ozone production and VOC reactivity in the atmosphere of the Mexico City Metropolitan Area. *Atmospheric Environment*, 238:117747, oct 2020. URL <https://doi.org/10.1016%2Fj.atmosenv.2020.117747>.
- [32] *Secretaría del Medio Ambiente (SEDEMA)*. URL <https://www.sedema.cdmx.gob.mx>. Accessed on Wed, December 02, 2020.
- [33] WHO, WMO, UNEP, and ICNIRP. Global solar UV index : a practical guide. Technical report, 2002.
- [34] Ann R. Webb, Harry Slaper, Peter Koepke, and Alois W. Schmalwieser. Know Your Standard: Clarifying the CIE Erythema Action Spectrum. *Photochemistry and Photobiology*, 87(2):483–486, jan 2011. URL <https://doi.org/10.1111%2Fj.1751-1097.2010.00871.x>.
- [35] C. D. Whiteman, S. Zhong, X. Bian, J. D. Fast, and J. C. Doran. Boundary layer evolution and regional-scale diurnal circulations over the and Mexican plateau. *Journal of Geophysical Research: Atmospheres*, 105(D8):10081–10102, apr 2000. URL <https://doi.org/10.1029%2F2000jd900039>.
- [36] J. D. Fast, B. de Foy, F. Acevedo Rosas, E. Caetano, G. Carmichael, L. Emmons, D. McKenna, M. Mena, W. Skamarock, X. Tie, R. L. Coulter, J. C. Barnard, C. Wiedinmyer, and S. Madronich. A meteorological overview of the MILAGRO field campaigns. *Atmospheric Chemistry and Physics*, 7(9):2233–2257, may 2007. URL <https://doi.org/10.5194%2Facp-7-2233-2007>.
- [37] *Sistema de Monitoreo Atmosférico (SIMAT)*. URL [www.aire.cdmx.gob.mx/default.php](http://www.aire.cdmx.gob.mx/default.php). Accessed on Wed, December 02, 2020.
- [38] B.N. Holben, T.F. Eck, I. Slutsker, D. Tanré, J.P. Buis, A. Setzer, E. Vermote, J.A. Reagan, Y.J.

Kaufman, T. Nakajima, F. Lavenu, I. Jankowiak, and A. Smirnov. AERONET—A Federated Instrument Network and Data Archive for Aerosol Characterization. *Remote Sensing of Environment*, 66(1):1–16, oct 1998. URL <https://doi.org/10.1016%2Fs0034-4257%2898%2900031-5>.

[39] NASA EOS/Aura Validation Data Center (AVDC) - Correlative data, Field of View Predictions, Data Subsets, GEOMS, DCIO. URL [https://avdc.gsfc.nasa.gov/pub/most\\_popular/overpass/OMI/](https://avdc.gsfc.nasa.gov/pub/most_popular/overpass/OMI/). Accessed on Wed, December 02, 2020.

[40] Saha Madronich. Intercomparison of NO<sub>2</sub> photodissociation and U.V. Radiometer Measurements. *Atmospheric Environment*, 21(3):569–578, jan 1987. URL <https://doi.org/10.1016%2F0004-6981%2887%2990039-4>.

[41] W. J. Shaw, M. S. Pekour, R. L. Coulter, T. J. Martin, and J. T. Walters. The daytime mixing layer observed by radiosonde profiler, and lidar during MILAGRO. *Atmospheric Chemistry and Physics Discussions*, 7(5):15025–15065, oct 2007. URL <https://doi.org/10.5194%2Facpd-7-15025-2007>.

[42] L. Elterman. An atlas of aerosol attenuation and extinction profiles for the troposphere and stratosphere. Technical report, dec 1966. URL <https://doi.org/10.21236%2Fad0649778>.

[43] C. A. Corr, N. Krotkov, S. Madronich, J. R. Slusser, B. Holben, W. Gao, J. Flynn, B. Lefer, and S. M. Kreidenweis. Retrieval of aerosol single scattering albedo at ultraviolet wavelengths at the T1 site during MILAGRO. *Atmospheric Chemistry and Physics*, 9(15):5813–5827, aug 2009. URL <https://doi.org/10.5194%2Facp-9-5813-2009>.

[44] T. Castro, S. Madronich, S. Rivale, A. Muhlia, and B. Mar. The influence of aerosols on photochemical smog in Mexico City. *Atmospheric Environment*, 35(10):1765–1772, apr 2001. URL <https://doi.org/10.1016%2Fs1352-2310%2800%2900449-0>.

[45] SEDEMA. Calidad del aire en la Ciudad de México, Informe 2017. Technical report, 2018a.

[46] Sergio Cabrera, Adriana Ipiña, Alessandro Damiani, Raul R. Cordero, and Rubén D. Piacentini. UV index values and trends in Santiago Chile (33.5°S) based on ground and satellite data. *Journal of Photochemistry and Photobiology B: Biology*, 115:73–84, oct 2012. URL <https://doi.org/10.1016%2Fj.jphotobiol.2012.06.013>.

[47] David D. Parrish, Hanwant B. Singh, Luisa Molina, and Sasha Madronich. Air quality progress in

North American megacities: A review. *Atmospheric Environment*, 45(39):7015–7025, dec 2011. URL <https://doi.org/10.1016%2Fj.atmosenv.2011.09.039>.

[48] *Informe anual calidad del aire 2017*. URL [http://www.aire.cdmx.gob.mx/descargas/publicaciones/flippingbook/informe\\_anual\\_calidad\\_aire\\_2017/mobile/#p=1](http://www.aire.cdmx.gob.mx/descargas/publicaciones/flippingbook/informe_anual_calidad_aire_2017/mobile/#p=1). Accessed on Thu, December 10, 2020.

[49] Molina, Velasco, Retama, and Zavala. Experience from Integrated Air Quality Management in the Mexico City Metropolitan Area and Singapore. *Atmosphere*, 10(9):512, aug 2019. URL <https://doi.org/10.3390%2Fatmos10090512>.

[50] Ronja Vitt, Gudrun Laschewski, Alkiviadis Bais, Henri Diémoz, Ilias Fountoulakis, Anna-Maria Siani, and Andreas Matzarakis. UV-Index Climatology for Europe Based on Satellite Data. *Atmosphere*, 11(7):727, jul 2020. URL <https://doi.org/10.3390%2Fatmos11070727>.

[51] Alexander Laskin, Julia Laskin, and Sergey A. Nizkorodov. Chemistry of Atmospheric Brown Carbon. *Chemical Reviews*, 115(10):4335–4382, feb 2015. URL <https://doi.org/10.1021%2Fcr5006167>.

[52] H. Gadhavi and A. Jayaraman. Absorbing aerosols: contribution of biomass burning and implications for radiative forcing. *Annales Geophysicae*, 28(1):103–111, jan 2010. URL <https://doi.org/10.5194%2Fangeo-28-103-2010>.

[53] Blanca Rios and Graciela B. Raga. Smoke emissions from agricultural fires in Mexico and Central America. *Journal of Applied Remote Sensing*, 13(03):1, sep 2019. URL <https://doi.org/10.1117%2F1.jrs.13.036509>.

[54] J. C. Barnard, R. Volkamer, and E. I. Kassianov. Estimation of the mass absorption cross section of the organic carbon component of aerosols in the Mexico City Metropolitan Area. *Atmospheric Chemistry and Physics*, 8(22):6665–6679, nov 2008. URL <https://doi.org/10.5194%2Facp-8-6665-2008>.

[55] B. Mayer, A. Kylling, S. Madronich, and G. Seckmeyer. Enhanced absorption of UV radiation due to multiple scattering in clouds: Experimental evidence and theoretical explanation. *Journal of Geophysical Research: Atmospheres*, 103(D23):31241–31254, dec 1998. URL <https://doi.org/10.1029%2F98jd02676>.